Available online at www.sciencedirect.com
ScienceDirect
Developmental Biology 303 (2007) 165–180
DEVELOPMENTAL BIOLOGY
www.elsevier.com/locate/ydbio

Defects in eye development in transgenic mice overexpressing the heparan sulfate proteoglycan agrin

Peter G. Fuerst, Steven M. Rauch, Robert W. Burgess *

The Jackson Laboratory, 600 Main Street, Bar Harbor, ME 04609, USA

Received for publication 29 June 2006; revised 10 November 2006; accepted 23 November 2006
Available online 2 December 2006

Abstract

The importance of heparan sulfate proteoglycans (HSPGs) in neurodevelopment is becoming increasingly clear. However, studies on HSPGs are hampered by pleiotropic effects when synthesis or modification of heparan sulfate itself is targeted, and by redundancy when the core proteins are altered. Gain-of-function experiments can sometimes circumvent these issues. Here we establish that transgenic mice overexpressing the HSPG agrin have severe ocular dysgenesis. The defects occur through a gain-of-function mechanism and penetrance is dependent on agrin dosage. The agrin-induced developmental defects are highly variable, and include anophthalmia, persistence of vitreous vessels, and fusion of anterior chamber structures. A frequently observed defect is an optic stalk coloboma leading to the misdifferentiation of the optic stalk as retina, which becomes continuous with the forebrain. The defects in optic-stalk differentiation correlate with reduced sonic hedgehog immunoreactivity and overexpansion of the PAX6 domain from the retina into the optic stalk. The ocular phenotypes associated with agrin overexpression are dependent on genetic background, occurring with high penetrance in inbred C57BL/6J mice. Distinct loci sensitizing C57BL/6J mice to agrin-induced dysgenesis were identified. These results indicate that agrin overexpression will provide a tool to explore the molecular interactions of the extracellular matrix and cell surface in eye development, and provide a means for identifying modifier loci that sensitize mice to developmental eye defects.

Keywords: Retina; *Pax6*; Sonic hedgehog; Heparan sulfate proteoglycan; Genetic modifiers; Development; Dysgenesis

Introduction

The functional importance of proteoglycans in a variety of developmental signaling events is well documented (Perrimon and Bernfield, 2000, 2001). Heparan sulfate proteoglycans (HSPGs) consist of a core protein with heparan sulfate (HS) post-translationally added to serine residues. Variations in the chemistry of this modification make it potentially extremely information dense (Turnbull et al., 2001) and the synthesis of HS is functionally critical for development. Eliminating HS synthesis in mice results in embryonic lethality at 6 days of gestation (E6) (Stickens et al., 2005). Tissue-specific deletion of HS synthesis in the nervous system results in numerous defects in morphogenesis and axon pathfinding (Inatani et al., 2003). In zebrafish, retinal axon sorting is affected by elimination of HS synthesis, though earlier developmental events may progress based on maternal contribution of mRNA, protein, and HS itself (Lee et al., 2004). More selective phenotypes are generated by chemical treatments or the elimination of enzymes that modify HS chains after they are synthesized (Bulow and Hobert, 2004; Grobe et al., 2005; Irie et al., 2002). The specificity of these effects has led to the hypothesis that a "Heparan code" exists, in which region-specific HS modifications encode spatial information required for neurodevelopment (Bulow and Hobert, 2004; Holt and Dickson, 2005).

Heparan sulfate influences many developmental signaling pathways, including Fibroblast growth factors (FGFs), Hedgehog (Hh), Wingless (Wnt) and Transforming growth factor β (TGF-β) (Baeg and Perrimon, 2000; Perrimon and Bernfield, 2000; Selleck, 2000). In addition to these broad developmental signaling systems, HS affects neuronal development and axon outgrowth through Semaphorin, LAR receptor tyrosine phosphatase, and Slit/Robo pathways (Fox and Zinn, 2005; Johnson et al., 2004; Kantor et al., 2004).

* Corresponding author. Fax: +1 207 288 6077.
E-mail address: Robert.Burgess@jax.org (R.W. Burgess).

0012-1606/$ - see front matter © 2006 Elsevier Inc. All rights reserved.
doi:10.1016/j.ydbio.2006.11.033

With their well-characterized anatomy and development, the developing eye and retina provide excellent models for the study of these pathways in morphogenesis, axon pathfinding and cell migration (Chow and Lang, 2001). In the mouse, eye development begins as an outgrowth of the telencephalon at approximately E8.5. This initiates a cascade of inductive events in which the neuroectoderm induces the surface ectoderm to become the lens. Through morphogenetic changes, the lens invaginates and subsequently induces the new surface ectoderm to become the cornea. In the process, the cup of invaginating tissue seals itself to become the eye. Retinal development continues into early postnatal life as the neuroepithelium differentiates, and the neurons migrate to their proper location within the retina, extend processes, and form synaptic connections.

The eye and other tissues express four primary families of HSPG. The syndecans and glypicans associate with the cell surface via transmembrane domains or glycosylphosphatidylinositol (GPI)-linkages, respectively (Bernfield et al., 1999; Park et al., 2000). Perlecan is an extracellular-matrix-associated HSPG, and agrin is primarily found in the extracellular matrix, though neurons also express a transmembrane isoform of the protein (Burgess et al., 2002; Neumann et al., 2001).

Agrin is most studied for its role in the development of the neuromuscular junction (NMJ) (Sanes and Lichtman, 1999), but it is also abundantly expressed in the eye. This expression suggests a possible function in eye development, although loss-of-function mutations in agrin do not cause an eye phenotype that is evident at birth, when the mice die from NMJ defects. In this study, we report that overexpression of agrin caused a variety of developmental eye defects, and that the penetrance of the defects was agrin-dose dependent. In addition, the defects were sensitive to genetic background and appeared in C57BL/6J with high penetrance. This allowed a modifier locus causing anophthalmia in the C57BL/6J background to be mapped to Chromosome 2. This report is the first demonstration of an overexpression phenotype for agrin, or any other HSPG, in the vertebrate eye, and presents a model through which biochemical and genetic interactions affecting neurodevelopment and morphogenesis may be studied. The model is also consistent with a role for HSPGs in multiple steps of eye development.

Materials and methods

Producing transgenic mice

A bacterial artificial chromosome (BAC) containing the entire *Agrn* gene, as well as 7 kb of upstream DNA and 30 kb of downstream DNA, was used to generate *Agrn* transgenic mice (BAC #19375, Genome Systems Inc, St. Louis, MO). *Agrn* is the only annotated gene on this BAC. The coding sequence of cyan fluorescent protein (CFP) was inserted into the last exon of *Agrn*, creating a fusion of CFP onto the C-terminus of *Agrn* using bacterial recombineering (Copeland et al., 2001; Lee et al., 2001). Two complementary primers, one matching the last 60 base pairs of the agrin coding sequence plus the first 20 base pairs of cyan fluorescent protein (CAG CTG CAT CTG CTG GAG GAC GCT GTC ACC AAA CCA GAG CTA AGA CCC TGC CCC ACT CTC ATG GTG AGC AAG GGC GAG GAG), and the other matching the first 60 base pairs of agrin's 3′ untranslated region and 20 base pairs of plasmid vector sequence (AAG TTT ACA AAA ATA GAA AAT AAT TAC AGG AGG GAA GGT GGC AGC TCT AGT GGC AGC TCA ACT CGA GCC CTT AAT TAA CCG GT), were used to amplify a CFP-loxP-FRT-TN5Neo-FRT cassette. The underlined portions of the oligos match the 5′ end of CFP and the complementary strand of the vector downstream of the Neo cassette. The loxP-frt-TN5Neo-frt plasmid was generously provided by Dr. Francis Stewart and allows positive selection with kanamycin in bacteria or neomycin in eukaryotic cells. This cassette was introduced into the agrin BAC by bacterial recombineering in EL250 *Escherichia coli*, and the selectable marker, TN5-Neo, was deleted from the BAC construct by expression of FLP to mediate recombination at the FRT sites.

Pronuclear microinjection was used to introduce the BACs into C57BL/6J embryos. Three independent founders were produced with integrated BAC constructs and expression levels of *Agrn-CFP* detectable by direct fluorescence. These strains are designated C57BL/6J-Tg(MGS1-19375/CFP)2R9Rwb, C57BL/6J-Tg(MGS1-19375/CFP)6R16Rwb and C57BL/6J-Tg(MGS1-19375/CFP)4R24Rwb, and are referred to hereafter as $Agrn^{CFP2R9}$, $Agrn^{CFP6R16}$, and $Agrn^{CFP4R24}$. The unmodified BAC 19375 was also used to generate a transgenic strain overexpressing *Agrn* without the CFP tag. This strain is designated C57BL/6J-Tg(MGS1-19375)72Rwb and is hereafter referred to as $Agrn^{72}$.

Animal husbandry

Mice were used in accordance with protocols approved by the Animal Care and Use Committee at The Jackson Laboratory. The Jackson Laboratory is accredited by AAALAC. Animals were housed in PIV caging and given food and water *ad libitum*.

Genetic rescue and Agrn dosage studies

For testing the functionality of the $Agrn^{CFP}$ transgenic strains and for reducing the dosage of *Agrn*, we used a deletion allele of *Agrn* generated by homologous recombination (Lin et al., 2001). This allele has the designation B6.129-$Agrn^{tm4Jrs}$/Rwb and is hereafter referred to as $Agrn^{Del}$. This strain deletes exons 6 through 33 of the agrin gene. However, an N-terminal fragment of agrin that is still produced and is recognized by antibodies such as GR14 (see below). Importantly, the N-terminal fragment produced is not glycanated, as predicted by sequence analysis searching for O-linked glycosylation consensus sequences and by empirical tests. This characterization was performed in collaboration with Dr. Jeffery H. Miner at Washington University and is submitted for publication.

Transgene integration sites

Chromosomal Fluorescence In-Situ Hybridization (FISH) was performed as previously described (Shopland et al., 2003). The *Agrn* BAC 19375 was labeled as a probe to identify the transgenic insertion sites. Fine mapping of the $Agrn^{CFP2R9}$ insertion site was performed by probing interphase nuclei of dispersed P5 hepatocytes with differentially labeled BACs, and assaying their orientation relative to each other. For this experiment the *Agrn* BAC was used in conjunction with two of the following BACs: RP23-114F11, RP24-263K11, RP24-168N14, RP24-511J6 and RP24-178B17 (CHORI). The $Agrn^{CFP2R9}$ transgene was found to have integrated in an intergenic region between RP24-168N14 and RP24511J6 on Chromosome 8. No effect on expression of flanking genes was observed, as assayed by real time PCR and northern blot analysis.

Genotyping of transgenic mice

Transgenic mice were genotyped using primers to CFP, or to the pBelo-BAC vector. To genotype the $Agrn^{CFP}$ transgenic strains, the primers XFP 5′ (ACC ATG GTG AGC AAG GGC) and XFP 3′ (CTT TAC TTG TAC AGC TCG TCC) were used. To genotype the $Agrn^{72}$ strain, the BAC-vector primers 400F (AGT GTC ACC TAA ATA GCT TG) and 900R (CAT GGG CAA ATA TTA TAC GC) were used. Tail biopsies were digested overnight in 100 µl of 1 mg/ml proteinase-K in 100 mM Tris pH 8.5, 10 mM EDTA, 200 mM NaCl buffer. Samples were then boiled for 15 min to denature the DNA and inactivate the proteinase-K. PCR was performed using master taq with the following program:

94 °C for 1 min, followed by 35 cycles of 94 °C for 20 s, 58 °C for 30 s and 72 °C for 2 min followed by a single 72 °C extension for 7 min (Eppendorf).

For Southern blot analysis, spleen was homogenized and digested with proteinase-K as above with the addition of 0.1% SDS. Samples were then phenol/chloroform extracted and precipitated with isopropanol. Genomic DNA was resuspended in water and digested with *Nco*I. Digestion products were run on a 0.8% agarose gel and transferred to Hybond membranes for blotting (GE Healthcare Life Sciences). An 800 bp probe generated by PCR from exon 35 to exon 36 of agrin was randomly primed using alpha-dCT^{32}P and hybridized to the membranes in Church buffer. High stringency washes were performed (final conditions of 0.2× SSC, 0.1% SDS at 65 °C).

Immunohistochemistry

Tissue was fixed in 4% paraformaldehyde for 4 h, rinsed in PBS, equilibrated overnight in PBS/30% sucrose for cryoprotection, and embedded in OCT media. Ten-micron cryostat sections of eyes or embryos were used for staining. Slides with sections were blocked in 1% BSA and 0.1% triton in PBS for 30 min. Primary antibodies were incubated on sections overnight at 4 °C, washed 4× 10 min in PBS and incubated with secondary antibodies for 1 h at room temperature. Slides were washed 4× 15 min in PBS. The last wash contained 1 μl of 1 mg/ml DAPI per 10 ml PBS. The following antibodies were used: rabbit anti-GFP, 1:500 (Chemicon); rabbit anti-PAX2, 1:1000 (Chemicon); mouse anti-PAX6, 1:25 NF clone 2H3, 1:1000; anti-SHH 1:50 (DSHB); rabbit anti-SHH 1:500 (Santa Cruz Biotechnology) and goat anti-CHX10, 1:500 (Santa Cruz Biotechnology). Sheep anti-agrin GR14 (1:800) was the generous gift of Dr. J.H. Berden, Radboud University Nijmegen Medical Center, The Netherlands. The specificity of this anti-agrin antibody was established by staining the kidney of a mouse strain completely lacking the isoform of agrin expressed in kidney (Burgess et al., 2000) and observing that all GR14 immunoreactivity was lost. Anti-mouse, -sheep, -rabbit and -goat secondary antibodies produced in donkey and conjugated with either Cy3 (Jackson Immunoresearch) or alexa-488 (Molecular Probes) were used to detect the appropriate primary antibodies at a dilution of 1:500.

Quantitative immunohistochemistry

Embryos were collected at E11.5, fixed for 2 h in 4% paraformaldehyde, and sucrose cryoprotected overnight at 4 °C. Embryos were frozen in OCT embedding media and cut in 10 μm sections, which were collected on slides such that an embryo of every genotype was represented on a single slide. Slides were blocked for 1 h in PBS supplemented with 3% normal horse serum and incubated overnight at 4 °C with antibodies to tubulin and agrin (Sigma-Aldrich). Primary antibodies were detected using a Cy3 labeled donkey anti-sheep antibody and an alexa-488 labeled goat anti-mouse IgG1 antibody (Jackson Immuno-Research and Molecular Probes, respectively). Slides were washed four times for 10 min in PBS and coverslipped. Images were acquired using a Leica SP5 confocal microscope with the same microscope parameters for all embryos. Agrin staining in the inner limiting membrane of the embryonic eye was imaged and normalized against tubulin staining in paraocular nerves. Three embryos (for a total of six eyes) were imaged for each genotype. Fluorescence intensity in the red and green channels was determined using the ImageJ RGB Measure Plugin.

Western blot analysis

Western blot analysis was performed on E11.5 embryo heads. 60 μg total protein was loaded in each lane. Blots were transferred to PVDF membranes and blocked in TBST (0.05% Tween) and 5% non-fat dry milk. Blots were probed using mouse monoclonal antibodies to GFP at a dilution of 1:4,000 (Invitrogen, clone 3E6) overnight at 4 °C followed by two 10 min washes at room temperature. Primary antibodies were detected using HRP labeled secondary antibodies at a dilution of 1:8,000, which were incubated for 1 h at room temperature (Perkin-Elmer, goat anti-mouse). All antibodies were diluted in TBS 0.05% Tween and 5% non-fat dry milk. Blots were stripped and reprobed with an antibody to MAP2 at a dilution of 1:2,000, which was used as a loading control (Chemicon). Four embryos of each genotype were examined. Densitometry was performed using ImageJ, and the ratio of anti-GFP to anti-MAP2 was determined for each lane. The mean ratio of CFP2R9, the highest expressing line, to MAP2 was chosen as 100%, and other ratios were expressed as a percentage of that value. Protein homogenates from the CFP2R9 strain were also treated with heparatinase (EC#4.2.2.8) or chondroitinase-ABC (EC#4.2.2.4) according to the manufacturers protocols (Seigaku), and blotted as described.

Transcript analysis

Isolation of RNA was performed using Trizol reagent according to manufacturer's instructions (Invitrogen). Messenger RNA was isolated by passage of total RNA over an oligo-dT cellulose column (Ambion). Two micrograms of mRNA from transgenic and wild-type mice was used per lane for northern blot analysis. The agrin probe was amplified by PCR from exon 21 to exon 25. First-strand cDNA was produced using a Superscript III first strand synthesis kit (Invitrogen) following the manufacturer's instructions with 5 μg of total RNA and a mix of dT and random hexamer primers used in each reaction. Quantitative real-time PCR was performed using the primers agrin F (GGT GCT GTG GAT TGG AAA GGT) and agrin R (TGC TGC GCT CCA CTG TGA) or beta-actin F (CAA CCG TGA AAA GAT GAC CCA GAT C) and beta-actin R (GAA TTG AAT GTA GTT TCA TGG ATG CCA C), with sybr green (ABI) for detection of amplification products.

Quantitative Trait Locus (QTL) analysis and mapping cross

Female mice from a BALB/cJ by C57BL/6J mating (CB6F1/J) were crossed to male *Agrn*^{CFP2R9} transgenic mice. At P28 mice were genotyped and eyes were enucleated and examined using a dissecting microscope. DNA was collected and purified from 100 *Agrn*^{CFP2R9} transgenic mice with various developmental defects. A genome-wide linkage analysis scan was performed by typing 140 strain specific single nucleotide polymorphisms (SNPs) spaced approximately every 10 mb along the chromosomes (K Bioscience). To establish significance thresholds for QTL testing, this data was used to simulate a whole-genome scan, performed at 5-cM spacing using 64 imputations and 100 permutations. These thresholds for the 1%, 5%, 10% and 63% significance levels are represented by the horizontal lines from greatest to smallest in each plot. QTL above the 1% threshold are considered strong QTL, while those above 63% are considered suggestive QTL (Doerge and Churchill, 1996; Sen and Churchill, 2001).

Results

Agrin transgenic mouse strains

Four strains of transgenic mice were generated by pronuclear injection of a BAC containing the *Agrn* gene into C57BL/6J embryos, as described in Materials and methods. Three of the four strains were made using a modified *Agrn* BAC producing enhanced cyan fluorescent protein (CFP) fused onto the C-terminus of agrin (*Agrn*^{CFP}, Fig. 1A). The fourth transgenic strain was made using the same agrin-containing BAC without CFP modification.

The deletion of agrin causes neonatal lethality, due to a failure of neuromuscular junction (NMJ) formation and maintenance. The transgenic *Agrn*^{CFP} strains *CFP2R9* and *CFP6R16* were capable of rescuing the lethality associated with deletion of *Agrn*, indicating that the transgenic protein is functional even with the CFP fusion. Staining NMJs with antibodies against neurofilament to visualize the nerve, and with rhodamine-conjugated α-bungaortoxin to visualize postsynaptic acetylcholine receptors, revealed no morphological differences between transgene-rescued and wild-type neuromuscular junctions (Figs. 1B, C, $N=3$). The transgenic agrin-CFP protein was detectable

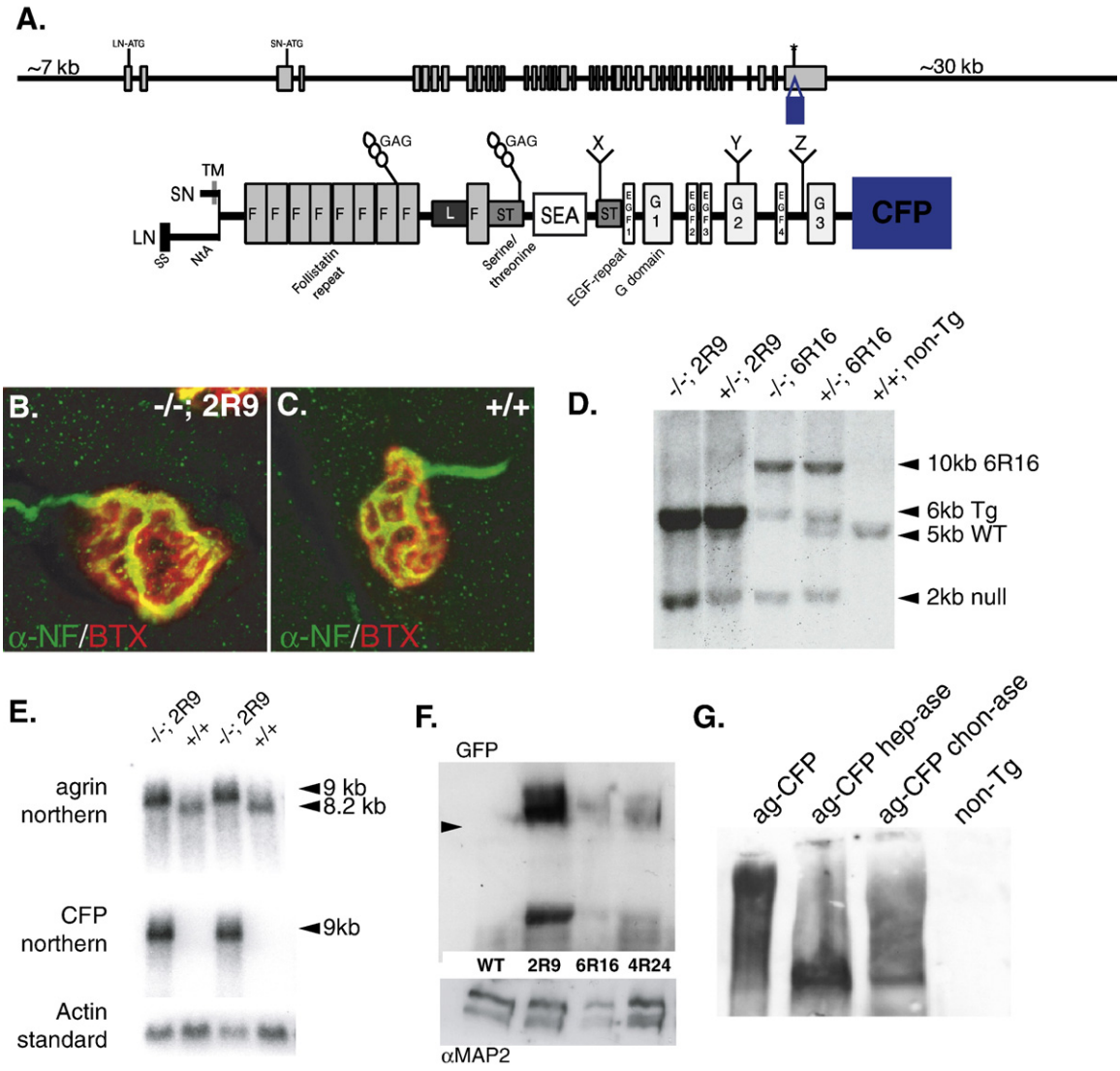

Fig. 1. Agrin transgenic mice. A) Agrin is a 40-exon gene spanning approximately 40 kb of genomic DNA. The agrin protein is almost 2000 amino acids long, with either a transmembrane N-terminus (SN-agrin) or an N-terminus with a signal peptide for secretion (LN-agrin). In the N-terminal half of the protein, there are nine-follistatin repeats (F), a laminin-like domain (L), two serine/threonine-rich regions (ST), and an SEA domain. In the C-terminal half, there are four EGF-like repeats (EGF) and three laminin-type globular domains (G). There are also at least three sites of alternative splicing (X, Y, Z). The sites of glycosaminoglycan (GAG) addition are in the N-terminal half of agrin. The agrin transgene construct was a BAC containing the entire agrin gene, in some cases modified to fuse cyan fluorescent protein (CFP) onto the C-terminus of agrin. B) The $Agrn^{CFP}$ transgene was functional and rescued the neonatal lethality caused by the deletion of agrin by homologous recombination. Mice homozygous for an agrin deletion, but carrying the transgene, had neuromuscular junctions (NMJs) that were indistinguishable from controls (C). The nerve, stained for neurofilament (green) overlapped the postsynaptic acetylcholine receptors labeled with α-bungarotoxin (red). The NMJs shown were from P12 mice. (D) The genotypes of mice rescued by the $Agrn^{CFP2R9}$ and $Agrn^{CFP6R16}$ transgenic strains were confirmed by Southern blotting. Digestion of genomic DNA with *Nco*I yielded the anticipated 2 kb band in the null allele, a 5 kb band in the wild-type allele, and a 6 kb band in the $Agrn^{CFP}$ transgene (caused by the CFP insertion). Lane 1 $Agrn^{Del/Del}$ rescued by the $Agrn^{CFP2R9}$ insertion, compared to an $Agrn^{Del/+}$littermate (lane 2). Lane 3 $Agrn^{Del/Del}$ rescued by the $Agrn^{CFP6R16}$ transgene, compared to an $Agrn^{Del/+}$ (lane 4). Lane 5 was a wild-type control. Notice the higher copy number of the $Agrn^{CFP}$ insertion in the 2R9 strain (dark 6 kb band). (E) Northern blotting confirmed that the only agrin transcripts generated in the rescued mice were the $Agrn^{CFP}$ from the transgene. The transgenic transcript was shifted by 1 kb by the CFP insertion. The same blots were hybridized with probes against Agrin, CFP, and *β-actin* as a loading control. Densitometry using a phosphorimager indicated that agrin was overexpressed approximately 2.5-fold in the 2R9 strain (shown in (E) at P12). F) The agrin-CFP protein was detectable by Western blotting using an anti-GFP antibody. The antibody did not recognize protein from non-transgenic mice (lane1), but recognized a high-molecular-weight smear in the $Agrn^{CFP}$ transgenic strains (arrowhead at 250 kDa). A smaller degradation or cleavage product was also evident, as previously reported for the endogenous protein. Relative expression levels of the $Agrn^{CFP}$ strains are shown, with MAP2 as a loading control shown below. G) The protein smear was reduced to a sharp band by treatment with heparatinase, and only partially affected by treatment with Chondroitinase ABC, consistent with the transgenic protein also being a heparansulfate proteoglycan.

at the NMJ using antibodies against GFP, and this staining was specific, as no anti-GFP immunoreactivity was seen in non-transgenic mice (not shown). Genotypes of the rescued mice were confirmed by Southern blotting (Fig. 1D). *Agrn* mRNA was analyzed by reverse-transcriptase PCR (RT-PCR) and northern blot analysis, which confirmed that the only *Agrn* expressed in the rescued mice was derived from the transgene (Fig. 1E). Densitometry of the northern blot compared to a *β-*

actin standard indicated a 2.5 fold overexpression of transgenic agrin transcripts in the *CFP2R9* strain. Agrin mRNA and protein expression levels were further examined by quantitative real-time PCR (qRT-PCR), quantitative immunofluorescence, and western blotting. The four transgenic lines expressed transgenic *Agrn* mRNA at levels 2.7, 2.4, 1.6 and 1.4 times higher than the endogenous gene by qRT-PCR and agrin transgenic protein at 3.3, 2.3, 1.2 and 0.8 times higher than endogenous protein levels by quantitative immunofluorescence (Table 1, $Agrn^{CFP2R9}$, $Agrn^{72}$, $Agrn^{CFP6R16}$, $Agrn^{CFP2R24}$ values respectively). The transgenic protein is detectable on a western blot using anti-GFP antibodies to recognize the C-terminal CFP fusion (Fig. 1F). Western blot analysis also showed protein levels of Agrn-CFP2R9 > Agrn-CFP6R16 > Agrn-CFP4R24 (Table 1). The agrin-CFP protein ran as a high molecular-weight smear, suggesting a glycoprotein. The smear was reduced to a band of approximately 275 kDa with heparitinase treatment and was less altered by digestion with chondroitinase ABC, consistent with the transgenic agrin-CFP being primarily a heparan sulfate proteoglycan (Fig. 1G).

Agrin overexpression disrupts eye development

The overexpression of agrin caused a phenotype specific to the eye. No overt neurological phenotypes such as tremor, seizures, or ataxia and no histological changes in the anatomy of agrin-rich tissues such as brain, muscle, or kidney were observed (not shown). Furthermore, no changes were observed in neuromuscular junction morphology, the site at which agrin's function is best documented. Indeed the original $Agrn^{CFP2R9}$ transgenic founder survived over 2 years. However, mice with high transgene expression levels had ocular dysgenesis with nearly complete penetrance. The two transgenic strains with highest *Agrn* expression had rates of ocular dysgenesis of 95% and 70% respectively (*CFP2R9* and *72*). The lines with lower transgenic expression of $Agrn^{CFP}$ (*CFP6R16* and *CFP4R24*) had an incidence of ocular dysgenesis similar to the spontaneous rate of occurrence in wild-type C57BL/6J mice (Table 1).

Table 1
Agrin transgene expression levels

Strain	*Agrn* vs. WT qRTPCR	Total agrin vs. WT QIF	Agrin-CFP vs. $Agrn^{CFP2R9}$ WBA	Percent dysgenic mice [a]
$Agrn^{CFP2R9}$	370±7.4%	434±78%	100±11%	95% (86/95)
$Agrn^{CFP6R16}$	260±18.2%	217±26%	44±8.7%	1% (1/88) [b]
$Agrn^{CFP4R24}$	240±7.2%	178±56%	25±5%	6% (3/54)
$Agrn^{72}$	340±17%	330±41%	NA	70% (42/60)
Wild-type [c]	100±4%	100±17%	NA	2% (2/106)

Levels of *Agrn* mRNA and agrin protein in transgenic mice. Four *Agrn* transgenic lines were analyzed for their agrin expression compared to the endogenous gene. Real time PCR was used to compare the level of transgenic *Agrn* mRNA expression to wild type littermates using *β-actin* as an internal control. Total agrin protein levels were determined and compared to wild type littermates by quantitative immunoflourescence, using anti-tubulin staining as a control. Agrin-CFP levels were measured in transgenic mice by western blot analysis, using MAP2 as a loading control. Levels of transgenic *Agrn* expression and protein were found to correlate with the penetrance of ocular dysgenesis. The $Agrn^{CFP2R9}$ line expressed the most *Agrn* and had the highest incidence of defects, followed by the $Agrn^{72}$ line. The $Agrn^{CFP6R16}$ line initially had an incidence of ocular dysgenesis of approximately 30% (11 of 31 mice), but after breeding, the incidence of dysgenesis approached the spontaneous level observed in wild-type C57BL/6J mice. The $Agrn^{CFP4R24}$ line expressed the lowest levels of *Agrn* and had an incidence of dysgenesis similar to wild-type C57BL/6J mice. The number of dysgenic mice over the total number of mice of each genotype analyzed is given.

qRT-PCR, Real-time PCR; QIF, Quantitative immunofluorescence; WBA, Western blot analysis.

[a] Mice were considered dysgenic if either of both eyes were developmentally abnormal based upon clinical examination.

[b] Eleven of thirty-one $Agrn^{CFP6R16}$ mice were dysgenic in the first generation, but rates fell to control values in subsequent generations as reported above.

[c] Wild-type mice are non-transgenic littermates of $Agrn^{CFP2R9}$.

The transgene insertions that caused eye defects with high penetrance are independent insertions. The genomic integration sites of the BACs were determined by FISH, and they were found to have integrated on different chromosomes (not shown), indicating the phenotype is not caused by a mutation created by the transgene insertion. In addition, one strain contains the CFP fusion ($Agrn^{CFP2R9}$) and the other is the unmodified agrin BAC ($Agrn^{72}$), indicating that the eye defects are not caused by the CFP.

The ocular dysgenesis correlated with the amount of *Agrn* expressed (Table 1). However, the phenotype could also be caused by the parallel expression of some other factor carried on the BAC. To test this, the level of *Agrn* expression was specifically decreased by crossing the high-expressing $Agrn^{CFP2R9}$ and $Agrn^{72}$ transgenic strains to an isogenic strain carrying an *Agrn* deletion ($Agrn^{Del}$, Chromosome 4) (Lin et al., 2001). Decreasing the dosage of *Agrn* by generating $Agrn^{Del/+}$ or $Agrn^{Del/Del}$ mice in an $Agrn^{CFP2R9}$ transgenic background reduced the incidence of dysgenesis to 56% of the mice heterozygous for the deletion, or 45% in mice homozygous for the deletion compared to 92% in wild-type littermates (Table 2). Similarly $Agrn^{72}$ in an $Agrn^{Del/+}$ background also reduced the incidence of eye defects to 56% from 73% in littermates. In $Agrn^{Del/Del}$ mice not carrying the $Agrn^{CFP2R9}$ transgene, examined at E18.5, 10 out of 11 examined had normal eyes, indicating that the ocular dysgenesis is not a part of the agrin loss-of-function phenotype (Table 2).

The reduction in agrin protein in the $agrn^{Del}$ allele was quantified by immunofluorescence. Fluorescence intensities in $Agrn^{Del/Del}$ mice were 64±14% that seen in wild-type mice, and the $Agrn^{CFP2R9}$; $Agrin^{Del/Del}$ mice were 318±28%, consistent with the reduced incidence of eye defects in $Agrn^{CFP2R9}$ mice mated to the $Agrn^{Del}$ allele. The $Agrn^{Del}$ allele expressed an N-terminal agrin fragment recognized by the antibody, although it is not glycanated and has no known activity (see Materials and methods). Thus, the decrease in penetrance of eye defects in $Agrn^{Del}$ backgrounds may be due to an even greater effective decrease in agrin protein levels than the staining indicates.

The ocular phenotypes observed in mice overexpressing *Agrn* are similar to those observed at a low spontaneous level in C57BL/6J and related Black strains such as C57BL/10, C58BL, and C57BL/Kahles. These defects range from anophthalmia to corneal–lenticular adhesions (Smith et al., 1994). The incidence and types of dysgenesis in mice carrying the highest-expressing transgene ($Agrn^{CFP2R9}$) was determined during embryonic development and in adults (Table 3). Most of the observed

Table 2
Effect of *Agrn* dosage on the penetrance of eye defects

Agrn genotype [a]	Transgene	Percent dysgenic [b]
Del/Del	Non-Tg	9% (1/11) [c]
Del/+	Non-Tg	3% (1/29)
+/+	Non-Tg	0% (0/15)
Del/Del	$Agrn^{CFP2R9}$	45% (4/11)
Del/+	$Agrn^{CFP2R9}$	56% (20/36)
+/+	$Agrn^{CFP2R9}$	92% (11/12)
Del/+	$Agrn^{72}$	56% (10/18) [c]
+/+	$Agrn^{72}$	73% (17/23) [c]

Agrn dosage effect. *Agrn* dosage was reduced by introducing $Agrn^{Del/+}$or $Agrn^{Del/Del}$ alleles into the $Agrn^{CFP2R9}$ or $Agrn^{72}$ backgrounds. Replacing a single wild-type allele in the $Agrn^{CFP2R9}$ line with the deletion reduced the incidence of dysgenesis from 92% to 56%, while being homozygous for the deletion reduced the incidence of defects to 45%. $Agrn^{72}$ mice carrying a single wild type allele of *Agrn* had a 17% decrease in the incidence of ocular dysgenesis. Littermate controls that did not carry an *Agrn* transgene had a very low incidence of dysgenesis; 2 mice out of 55 not carrying an *Agrn* transgene had malformed eyes, consistent with the background incidence of these defects. Importantly, the $Agrn^{Del/Del}$ mice did not have dysgenic eyes, consistent with the phenotype not being part of the *Agrn* loss-of-function phenotype.

[a] The *agrn* genotype at the endogenous Chromosome 4 locus.

[b] A mouse was scored as dysgenic if one or both eyes had any developmental phenotype by clinical and histological examination.

[c] $Agrn^{Del/Del}$; Non-Tg mice and $Agrn^{72}$ were collected at E18.5.

phenotypes fell into three categories: 1) fusion of anterior chamber structures, 2) pigmented persistent hyperplastic primary vitreous (PHPV) associated with a failure to close the fetal fissure, and 3) coloboma and misdifferentiation of the optic stalk. Examples of these phenotypes are shown in Supplemental Fig. 1. The first two categories of phenotype are spontaneous defects normally observed at low frequency in C57BL/6J and related strains, while the third has not been described in C57BL/6.

Localization of transgenic and wild-type agrin in the eye

To determine whether the transgenic agrin-CFP protein has wild-type localization or is ectopically expressed within the eye, transgenic and wild-type eye sections were stained using antibodies directed against agrin (GR14) to detect endogenous and transgenic agrin (Raats et al., 1998), and against GFP, which cross reacts with CFP, to detect transgenic agrin-CFP.

Distribution of agrin in sections of wild-type eyes was identical to the distribution of agrin-CFP in transgenic eyes, indicating that transgenic agrin-CFP is not ectopically localized in the eye (Figs. 2A–D, data not shown). Agrin-CFP in the retina was localized to the internal limiting membrane, to cells at the boundary of the inner plexiform layer, to the inner nuclear layer, and to the outer plexiform layer (Figs. 2B, D). Double labeling experiments were performed to identify the agrin-CFP-positive cell populations. No significant co-localization of agrin-CFP with PAX6 (a marker of amacrine, ganglion and horizontal cells) or with vimentin (a marker of Mueller glia) was observed. However, agrin-CFP did co-localize with laminin, a marker of endothelial cells, which identified these cells as part of the retinal vasculature (Fig. 2E, data not shown). Outside the neural retina, agrin-CFP was localized to the basal lamina of several distinct structures in the adult eye, including retinal vasculature, the internal limiting membrane, the lens capsule, the ciliary body and the iris, as well as Descemet's membrane and Bowman's layer of the cornea (Figs. 2F–H). In the optic nerve, agrin-CFP was localized to the outer sheath of the nerve and was not detectable on axons in adult samples (Fig. 2I).

In the developing eye, agrin-CFP was localized along the neural ectoderm and surface ectoderm at E9.5, the outer face of the optic cup, the interior surface of the optic stalk and the interior invaginating lens capsule at E10.5 and E12, and the hyaloid vessels at E14 (Figs. 3A–D). As in adult mice, transgenic agrin-CFP distribution was identical to that of agrin in the wild-type eye, as determined using the GR14 antibody to agrin (Figs. 3E, F). Since localization of wild-type and transgenic agrin overlapped completely, detection of transgenic agrin in the rest of this study was performed using antibodies to GFP.

Agrin-CFP localizes to dysgenic structures

To assess whether the effect of agrin overexpression on eye development could be a direct consequence of the presence of the transgenic protein, the localization of agrin-CFP was assayed in eye structures at times corresponding to the initiation of dysgenesis. Direct effects of agrin-CFP could include the altered presentation of growth factors or changes in cell adhesion or migration that are normally mediated by the ECM within the eye. Indirect effects could include factors that

Table 3
Prevalence of dysgenesis in $Agrn^{CFP2R9}$ transgenic mice

Dysgenesis [a]	E9.5	E10.5	E12.5	E14–16	P0	P21
PHPV	NA [b]	NA	NA	NA	59% (10/17)	51% (109/214)
Iridocorneal adhesion	NA	NA	NA	NA	12% (2/17)	11% (24/214)
Corneal–lenticular adhesions	NA	NA	80% (12/15)	70% (7/10)	82% (14/17)	75% (161/214)
Iris/fetal fissure coloboma [c]	NA	NA	40% (6/15)	34% (21/62)	18% (3/17)	15% (32/214)
Microphthalmia	NA/ND	NA/ND	NA/ND	NA/ND	NA/ND	3% (7/214)
Anophthalmia	NA/ND	NA/ND	13% (2/15)	3% (2/62)	6% (1/17)	37% (79/214)
Optic cup orientation	(0/11)	72% (8/11)	NA	NA	NA	NA

Prevalence of dysgenesis in $Agrn^{CFP2R9}$ transgenic mice. Dysgenesis was evaluated at different developmental stages in transgenic mice. Both eyes of each mouse were scored; numbers reported represent mice. A given mouse could fall into multiple categories if different phenotypes were present in each eye.

[a] Numbers represent mice. Both eyes of a given mouse were evaluated.

[b] ND = Not determined, NA = Not applicable.

[c] Includes coloboma and misdifferentiation of the optic stalk.

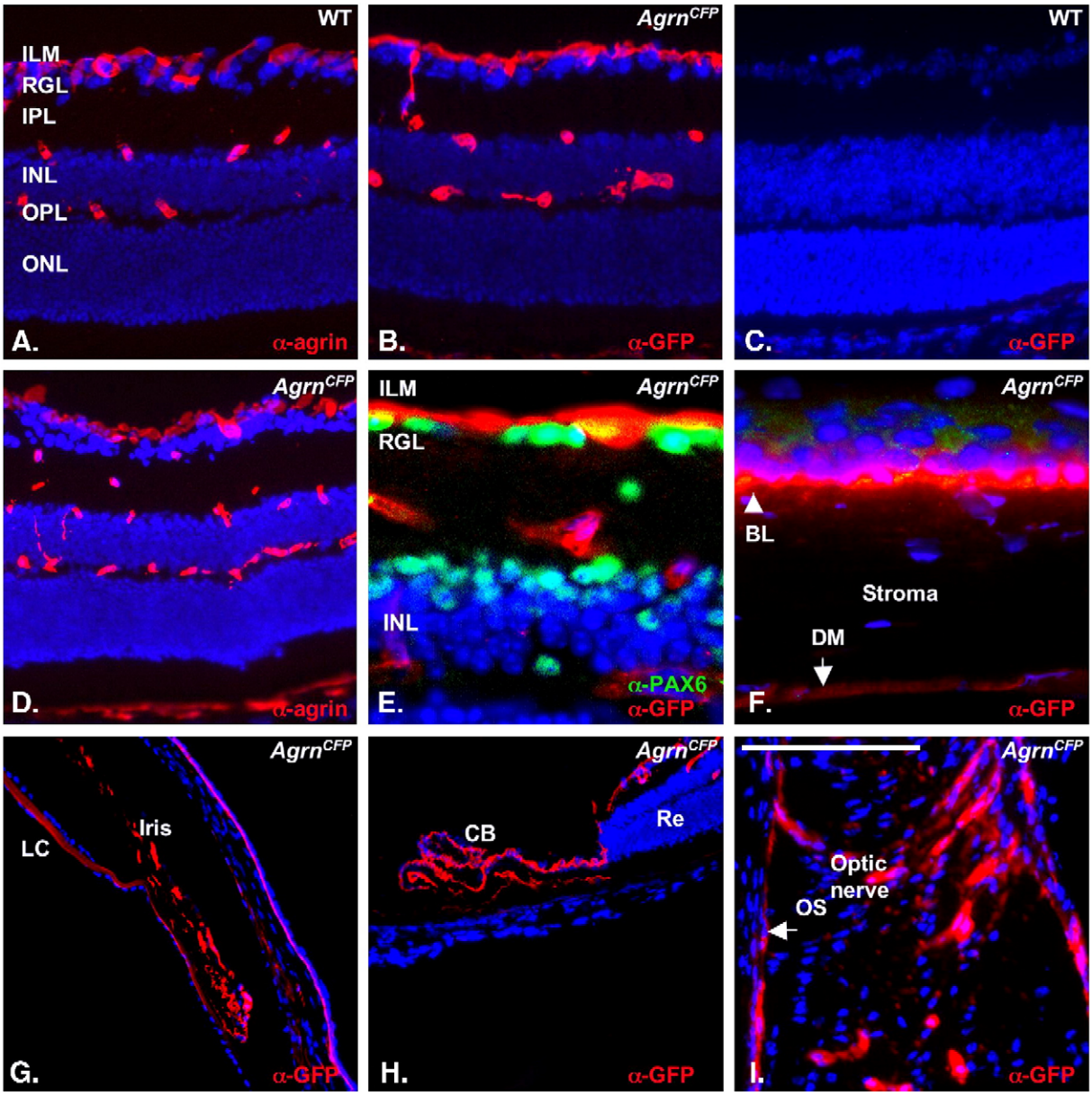

Fig. 2. Distribution of agrin and agrin-CFP in the adult mouse eye. (A) Cross sections of wild type retinas stained with anti-agrin antibodies (GR14, red) revealed agrin to be localized to cells on the edges of the inner nuclear layer (INL) and outer plexiform layer (OPL), which were identified as blood vessels, and along the internal limiting membrane (ILM). The photoreceptors of the outer nuclear layer (ONL) were not labeled. (B) Cross sections of *Agrn*^{CFP6R16} retinas labeled using an anti-GFP antibody to recognize the transgenic protein (red), showed agrin-CFP localization to be identical to anti-agrin on wild-type sections. (C) Transverse sections of wild-type eyes stained with anti-GFP antibodies showed no staining, establishing that the antibody is specific for the transgenic agrin-CFP protein. (D) Sections of transgenic retinas stained with the GR14 anti-agrin (red) revealed the same localization. (E) Transverse sections of transgenic retinas probed with antibodies to GFP (red) and PAX6 (green) revealed that agrin-CFP does not co-localize with PAX6. (F) In the cornea, agrin-CFP is localized to Descemet's membrane (DM) and Bowman's layer (BL). (G, H) In the anterior chamber of the eye, agrin-CFP is localized to the iris (I), ciliary bodies (CB) and lens capsule (LC). (I) Sections of optic nerve from *Agrn*^{CFP6R16} mice showed agrin-CFP localization to the outer sheath (OS) of the nerve, which is continuous with the blood–brain barrier. Retinal sections are oriented with the retinal ganglion layer (RGL) up. All sections are counter-stained with DAPI (blue) to visualize nuclei. The measurement bar located in the lower right panel is equivalent to 75 μm in A, B, C, F and H, 225 μm in D and E, and 37.5 μm in G and I.

increased fetal stress, which can exacerbate the propensity of C57BL/6J to develop abnormal eyes, as seen in fetal alcohol exposure (Sulik et al., 1981).

Agrin-CFP was indeed present in structures that become malformed, immediately preceding and following the initiation of dysgenesis. The lens stalk connecting the developing lens to the overlying surface ectoderm typically is lost through an apoptotic mechanism by E12 in wild-type mice. Agrin-CFP is localized to the basal lamina of the lens stalk in E11.5 embryonic samples. In E14 samples, agrin-CFP was in the fetal fissure (Fig. 4B), which closes by E12 in wild-type embryos, but frequently persisted in the transgenic eyes. The open fissure may contribute to the infilitration of fibrovascular tissue observed later. Coloboma and misdifferentiation of the optic

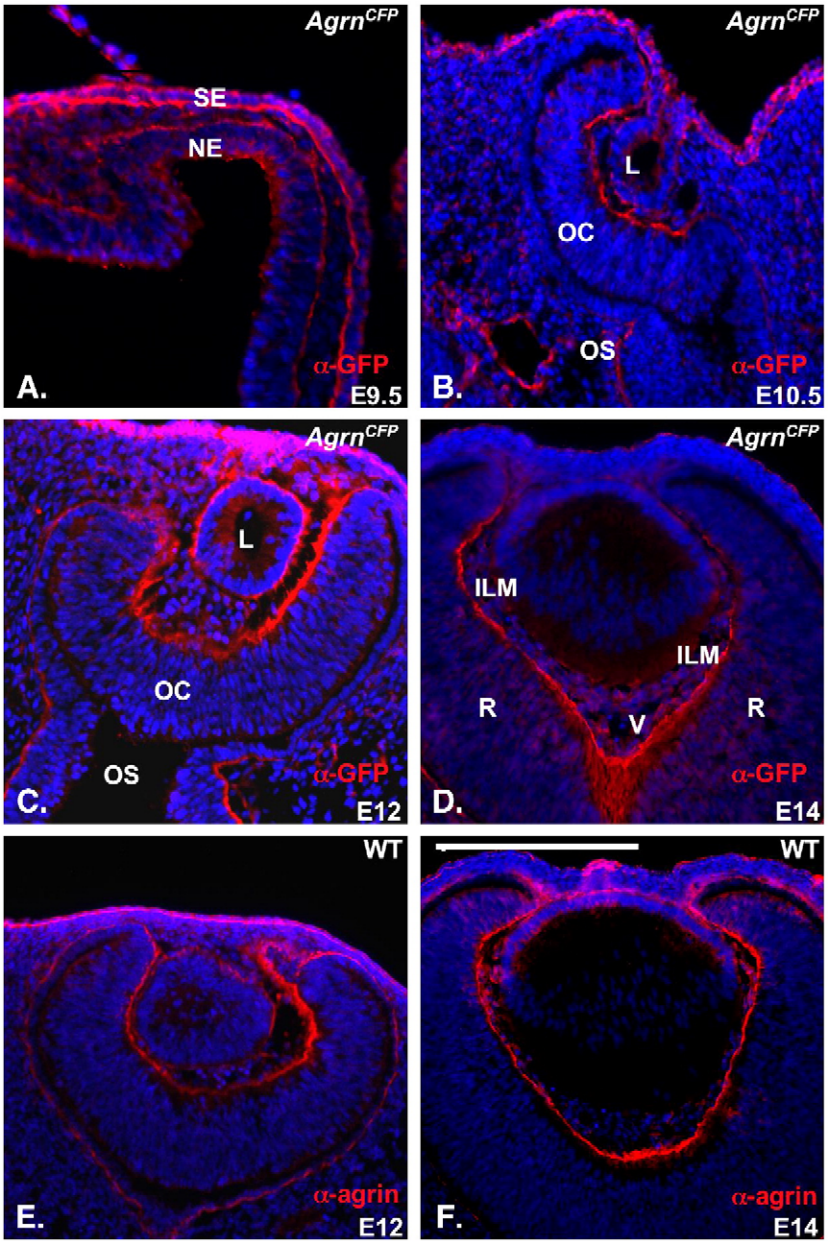

Fig. 3. Agrin and agrin-CFP localization in the developing eye. The presence of agrin in the developing eye was assayed at four times relevant to the onset of developmental defects observed in dysgenic eyes. (A) In E9.5 $Agrn^{CFP6R16}$ embryos stained with antibodies to GFP, agrin-CFP is localized to the ECM separating the neural and surface ectoderm (NE and SE). (B) In E10.5 transgenic embryos, agrin-CFP is localized to the ECM of the interior optic cup (OC) and surrounding the invaginating lens (L), as well as along the exterior optic stalk (OS). (C) In E12 transgenic embryos, agrin-CFP is present in the ECM of the optic cup (OC), lens capsule (L) and inner and outer optic stalk (OS). (D) In E14 transgenic embryos agrin-CFP is localized to the vitreous (V) and internal limiting membrane (ILM) of the retina (R). Sections of wild-type eyes at E12 (E) and E14 (F) were stained with an anti-agrin antibody (GR14, red). The distribution of agrin in the wild-type developing eye is the same as the distribution of transgenic agrin-CFP in $Agrn^{CFP6R16}$ transgenic mice. All sections are counterstained with DAPI (blue) to visualize the nuclei. The measurement bar located in the lower right panel is equivalent to 165 μm in A, 210 μm in B and 250 μm in C–F.

nerve was observed in up to 40% of embryos at E15–E16. The entire dorsal optic nerve differentiates as retina in affected embryos, as determined by histology and the expression of the retina-specific marker CHX10 (Figs. 4C, D). Agrin-CFP is abundantly localized to the surface of the misdifferentiated optic nerve. Maintenance of the boundary between the optic cup and the optic stalk is mediated by restriction of *Pax6* expression to the optic cup, while PAX2 is found in the developing nerve in wild-type embryos. In dysgenic $Agrn^{CFP2R9}$ eyes, PAX6 is localized to the misdifferentiated dorsal optic nerve, while PAX2 is localized to the ventral optic nerve (Fig. 4E). In neonatal mice, an acellular ECM, containing agrin-CFP and dystroglycan, connected the lens and cornea of the transgenic eye (Fig. 4F). Agrin-CFP was also localized to the hyaloid vessels, which adhere to the surface of the retina (Fig. 4G). After eye opening in mice with a fusion of either the lens or the iris with the cornea, agrin-CFP was found in endothelial tissue bridging adhesions (Figs. 4H, I).

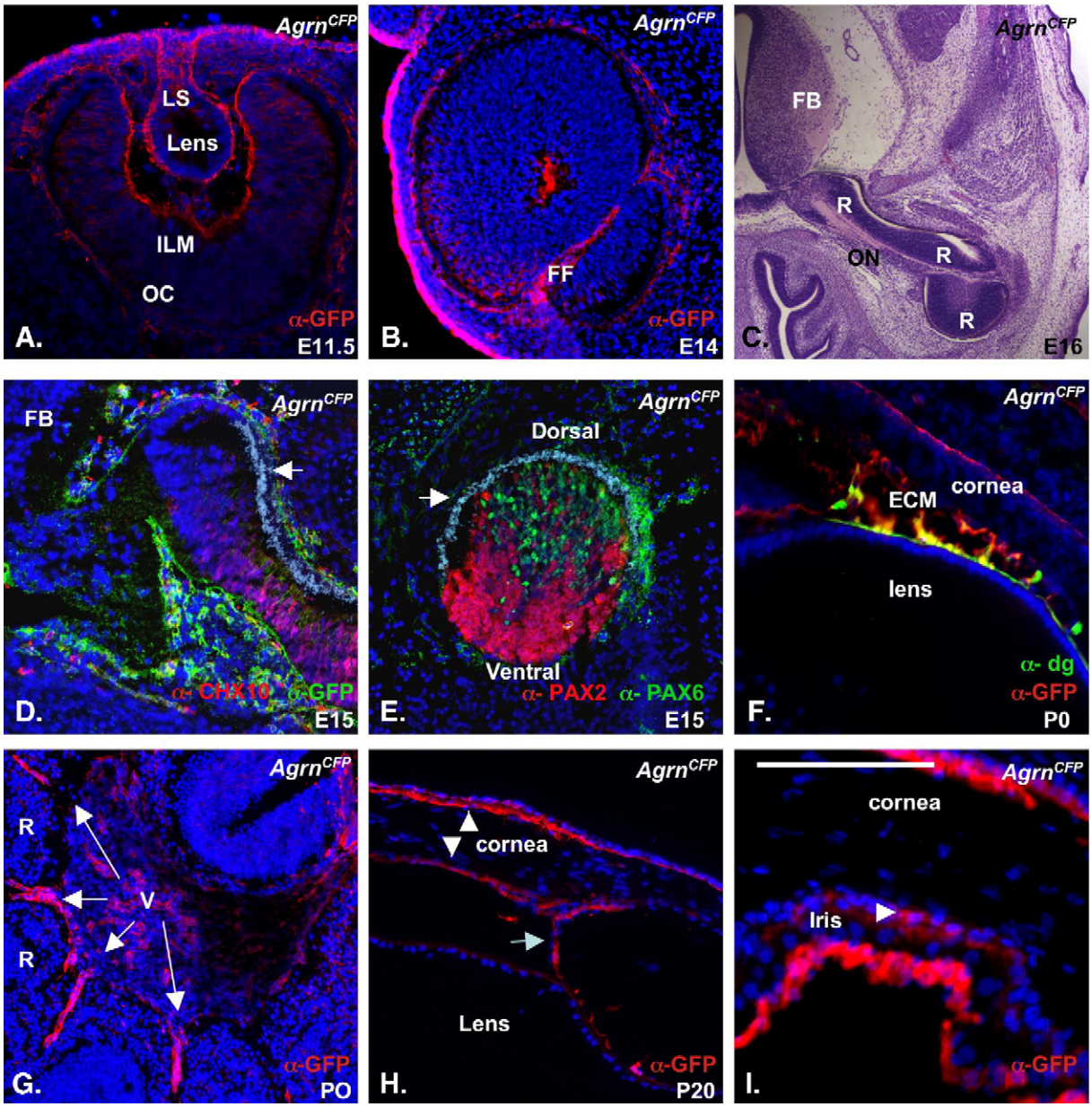

Fig. 4. Agrin-CFP localization in the dysgenic eye. (A) In E11.5 $Agrn^{CFP2R9}$ eyes stained with antibodies to GFP (red), agrin-CFP is localized throughout the lens stalk (LS), as well as along the basal lamina of the surface epithelium and lens, and the internal limiting membrane (ILM) of the optic cup (OC). (B) Transverse sections through the ventral optic cup of E14 $Agrn^{CFP2R9}$ eye revealed agrin-CFP to be localized to the persistent fetal fissure (FF). (C) Transverse sections through E16 $Agrn^{CFP2R9}$ embryos stained with hematoxylin and eosin revealed misdifferentiation of retinal tissue along the length of the optic nerve. The retina (R) formed in place of the dorsal portion of the optic nerve (ON), and is continuous with the forebrain (FB). (D) E15 $Agrn^{CFP2R9}$ optic nerve sections were stained with antibodies to GFP, to detect agrin-CFP (green), and CHX10 (red), a marker of retinal differentiation. The retinal pigment epithelium, visualized with brightfield microscopy, is marked on the image (arrow). CHX10 labeled the misdifferentiated tissue, and agrin-CFP is localized to the ECM surrounding the optic nerve. (E) Sagittal sections of E15 $Agrn^{CFP2R9}$ optic nerves were stained with antibodies to PAX6 (green) and PAX2 (red), PAX6 localized to the dorsal half of the optic nerve, while PAX2 localized to the ventral half. The retinal pigment epithelium is again marked (arrow). (F) In P0 $Agrn^{CFP2R9}$ eyes double-labeled with anti-GFP to detect agrin-CFP (red) and dystroglycan (green), agrin-CFP co-localizes with dystroglycan in acellular ECM connecting the lens and cornea. (G) In P0 $Agrn^{CFP2R9}$ eyes with infiltration of fibrovascular tissue, agrin-CFP localized to hyaloid vessels (V) adhering to folds of the retina (R). (H) In P20 $Agrn^{CFP2R9}$ eyes with lens–cornea fusions, agrin-CFP localized to the basal lamina of the cornea (arrow heads) and to tissue connecting the lens and cornea (arrow). (I) In P20 $Agrn^{CFP2R9}$ eyes with irideocorneal fusion, agrin-CFP is localized to the points of adhesion between the iris and cornea (arrowhead). The measurement bar located in the lower right panel is equivalent to 90 μm in A, 250 μm in B, 1.1 mm in C, 220 μm in D and E, 105 μm in F, 180 μm in G, 75 μm in H, and 35 μm in I.

Developmental pathways affected by agrin overexpression

To further define the developmental pathways perturbed by agrin overexpression, the PAX2/PAX6 boundary defects (Figs. 4C–E) were further examined. The *Pax2* and *Pax6* expression domains underlie optic nerve and retinal differentiation respectively, and defects in the boundary between the domains cause optic nerve misdifferentiation in other models (Mui et al., 2005; Take-uchi et al., 2003). Immunohistochemistry was performed on sections of wild-type and transgenic mice at two

embryonic stages to identify the age at which the PAX2/PAX6 boundary became abnormal. The developing eyes of transgenic and wild-type mice had similar patterns of PAX2 and PAX6 localization at E12, despite the morphological abnormality of transgenic eyes at this point (Figs. 5A–C, $N=5$). However, by E14, PAX6 had expanded into the optic nerve of $Agrn^{CFP2R9}$ mice, particularly in the dorsal portion of the nerve ($N=3$) (Figs. 5D–F).

Sonic hedgehog (SHH), which maintains repression of *Pax6* in the optic stalk, was monitored at E11.5 in the midbrain and at E12.5 and E14 at the optic disk ($N=2$, 5 and 3 respectively), to assess whether a change in the distribution of this molecule correlated with expansion of the PAX6 domain in the *Agrn*- optic nerve. The SHH staining pattern and intensity was similar in transgenic and control embryos in the midbrain at E11.5, or at the posterior optic cup at E12.5 (Fig. 6A–D). However, by E14, widely varying staining of SHH that was less intense than wild type was observed in $Agrn^{CFP2R9}$ mice (Figs. 6E, F).

Retinal ganglion cells in $Agrn^{CFP2R9}$ retinas, identified by expression of BRN3b (POU4f2), were apparent by E13, indicating that a decrease in SHH levels in the developing optic nerve was not caused by a failure of retinal ganglion cell neurogenesis (data not shown). However, the lower levels of SHH could have been from a decrease in the number of axons navigating down the developing nerve. To assess the number of RGC axons associated with the optic nerve, cross sections were stained with an antibody to neurofilament (NF), and PAX2. Compared to wild type, the optic nerve of transgenic mice with optic nerve colobomas had markedly less neurofilament immunoreactivity along the ventral portion of the optic nerve, and the cross-sectional area was considerably larger than in wild type, because of the coloboma (Figs. 6G–J, N3 transgenic and WT).

Distinct loci underlie C57BL/6J sensitivity to Agrn overexpression

The ocular dysgenesis observed in *Agrn* overexpressing C57BL/6J mice closely resembled the low incidence of defects that occur spontaneously in this inbred strain, suggesting that C57BL/6J is sensitized to the defects induced by *Agrn* overexpression. Ocular dysgenesis was observed in F1 *Agrn*- mice derived from crosses to closely related strains (C57BL/10J, C57BL/6J, C57BR/cdJ and C57BL/6ByJ), but was not observed in F1 mice from crosses to more distantly related inbred strains, including C3H/HeJ, BALB/cJ, DBA/2J and SJL/J. Backcrossing the latter F1 mice to C57BL/6J, or intercrossing the F1 progeny, resulted in varying degrees and penetrance of ocular defects, indicating the presence of recessive sensitivity loci in C57BL/6J and possibly dominant repressors in the non-C57BL/6J strains. Expression levels of $Agrn^{CFP2R9}$ in different genetic backgrounds did not change, as measured by qRT-PCR,

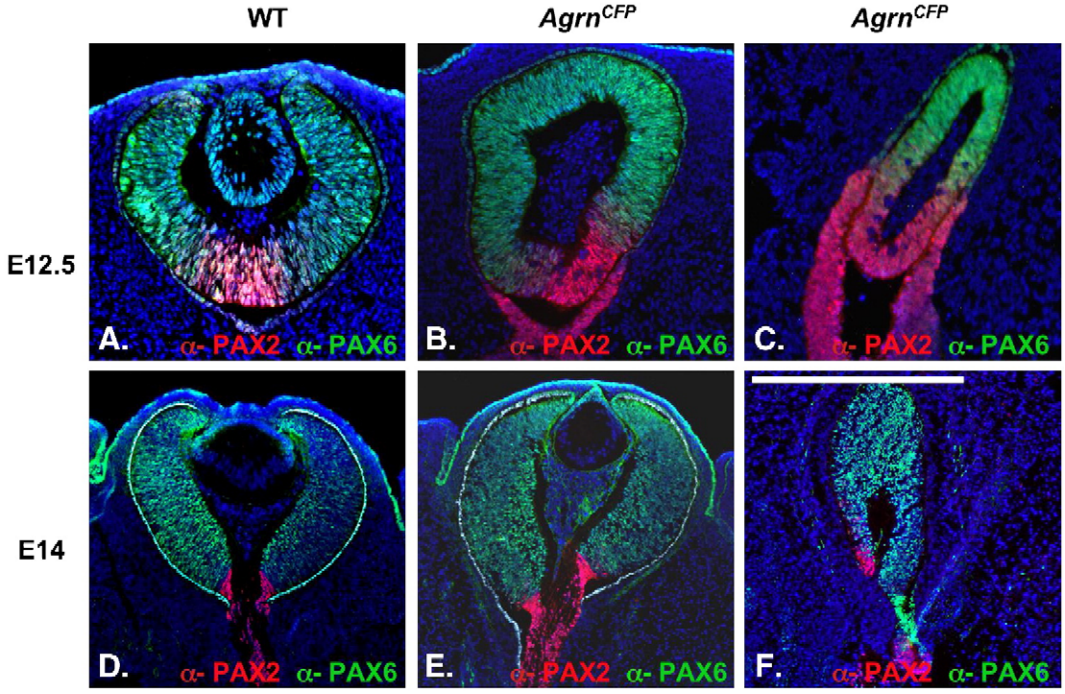

Fig. 5. PAX2 and PAX6 localization in $Agrn^{CFP2R9}$ and wild-type eyes during development. Embryonic eyes at E12.5 and E14 were labeled with antibodies to PAX2 (red) and PAX6 (green). Mildly affected and severely affected examples of $Agrn^{CFP2R9}$ eyes are shown in the middle column and right column respectively. (A) In wild-type embryos at developmental day 12.5, PAX6 is localized to the peripheral optic cup, while PAX2 is limited to the posterior margin of the optic cup. (B and C) In $Agrn^{CFP2R9}$ eyes at developmental day E12.5, PAX2 and PAX6 localization is similar to that of the wild-type eye; PAX6 is limited to the optic cup and PAX2 is localized to the posterior margins of the optic cup and optic stalk, regardless of the degree of dysgenesis. (D) At E14, PAX6 is localized to the optic cup, while PAX2 is localized to the optic nerve in wild-type eyes. (E) In mildly dysgenic $Agrn^{CFP2R9}$ eyes at E14, PAX6 and PAX2 localization was similar to wild-type, with PAX6 limited to the optic cup, and PAX2 limited to the optic nerve. (F) However, in severely dysgenic $Agrn^{CFP2R9}$ eyes with optic nerve colobomas, PAX6 localization expanded medially along the dorsal optic nerve, while PAX2 localized to the ventral margin of the medial optic nerve. The measurement bar located in the lower right panel is equivalent to 215 μm in A–C and 415 μm in D–F.

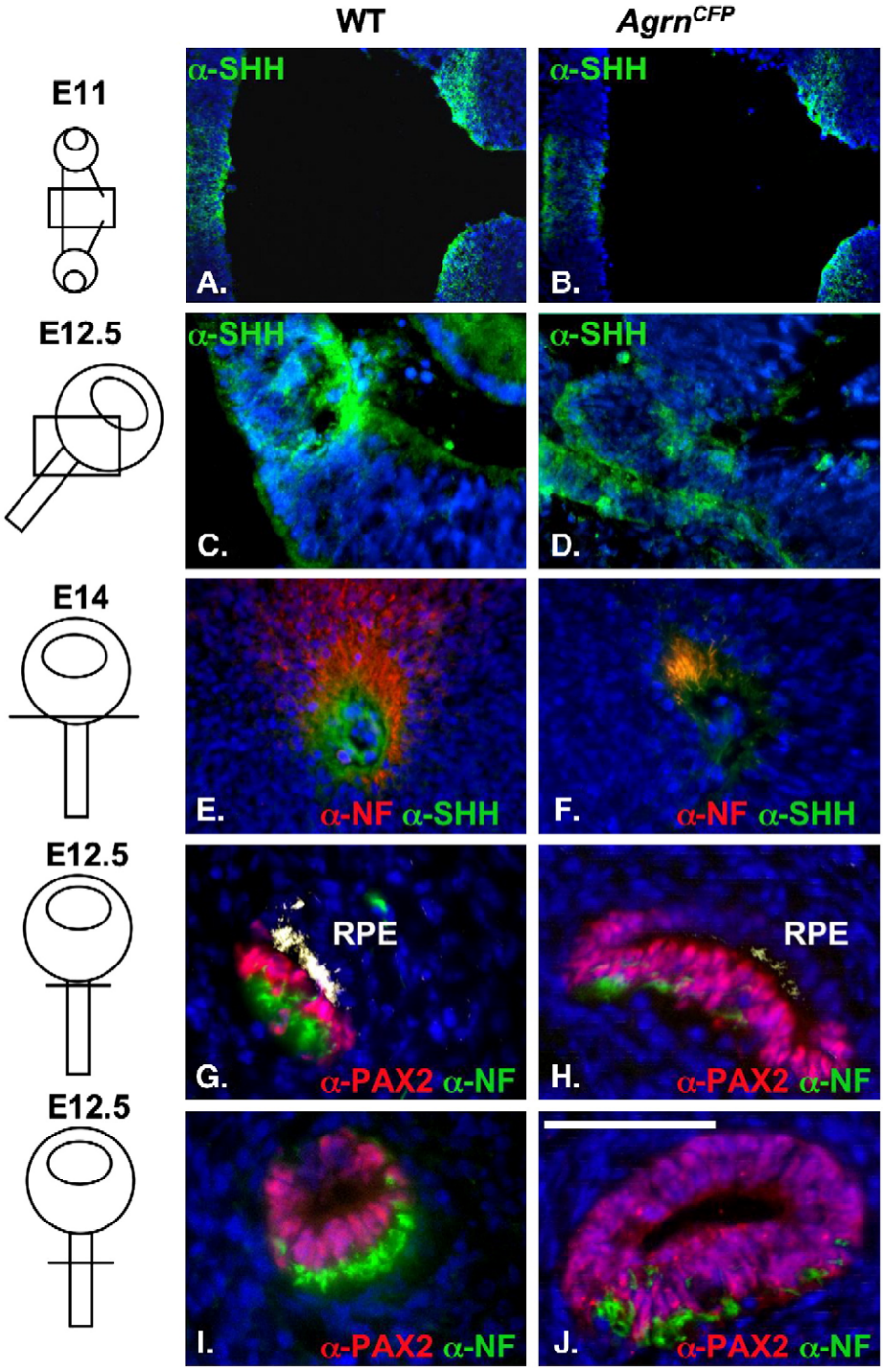

Fig. 6. SHH and optic nerve development in *Agrn*^{CFP2R9} mice. The schematics in the left column represent the planes of section and regions of interest for each pair of images, shown in relation to the developing eyes and optic nerve. (A and B) Transverse sections of wild-type and *Agrn*^{CFP2R9} E11 embryos stained with antibodies to SHH (green) revealed a similar midline and parasagittal staining pattern in the telencephalon. (C and D) Transverse sections of E12.5 embryos stained with antibodies to SHH (red) showed a similar staining intensity in *Agrn*^{CFP2R9} mice compared to controls. (E and F) Wild-type and *Agrn*^{CFP2R9} E14 embryos sectioned at the optic disc and double-labeled with antibodies to SHH (green) and neurofilament (NF, red) showed varying levels of SHH in *Agrn*^{CF2R9P} mice, ranging from nearly wild type to vastly reduced (an intermediate example is shown in F). (G–J) Sagittal sections at the optic disc (G, H) or in the developing optic nerve (I, J) from E12.5 embryos were stained with antibodies to NF (green) and PAX2 (red) to visualize the retinal ganglion cell axons and the cells of the optic stalk, respectively. NF staining was reduced in the *Agrn*^{CFP2R9} transgenic optic nerve compared to wild-type. The cross-section of the optic nerve of *Agrn*^{CFP2R9} embryos was also much larger compared to wild type controls, reflecting the failure of the optic stalk to fuse. The measurement bar located in the lower right panel is equivalent to 280 μm in A and B, 98 μm in C and D, 95 μm in E and F, 70 μm in G and H and 50 μm in I and J.

indicating that expression of agrin is not strain-dependent and therefore could not explain the strain-specificity of dysgenesis (not shown).

A genetic mapping cross was performed to identify chromosomal regions associated with ocular dysgenesis in C57BL/6J mice overexpressing *Agrn*^{CFP2R9}, and linkage

analysis was performed. Treating all forms of dysgenesis as a single phenotype with varying severity did not yield any significant linkage in whole-genome scans (Fig. 7A). A suggestive locus was observed on Chromosome 13, and nearly suggestive loci were observed linked to Chromosomes 2, 4 and 11. If the model of a single eye phenotype with varying severity in C57BL/6 mice overexpressing *Agrn* is accurate, then the phenotype is the result of multiple interacting genomic loci, each of which has a weak effect on the phenotype.

To model an alternative hypothesis, in which the dysgenesis observed in $Agrn^{CFP2R9}$ mice is a group of distinct phenotypes affecting eye development at discrete steps, the mice genotyped

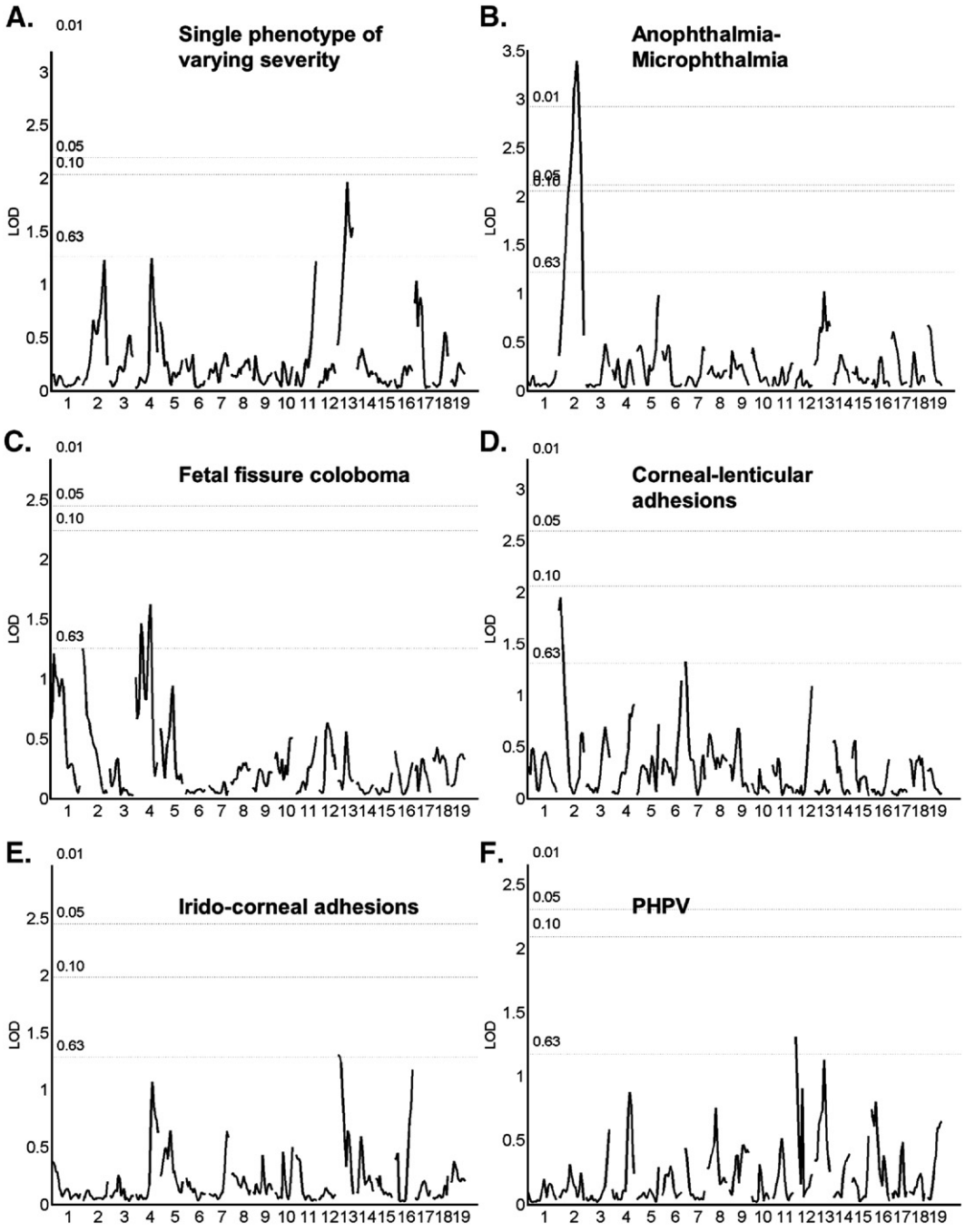

Fig. 7. QTL maps of C57BL/6J loci associated with ocular dysgenesis. A plot of the log of odds (lod) that a given chromosomal location would segregate in the cross at observed levels in dysgenic mice. Chromosome numbers are plotted along the *X*-axis with the centromeric end to the left. The log of odds is plotted on the *Y*-axis. (A) Modeling the various types of ocular dysgenesis observed in $Agrn^{CFP2R9}$ mice as a continuous spectrum of a single phenotype identified a single suggestive locus on Chromosome 13. The ocular defects observed in $Agrn^{CFP2R9}$ mice were therefore also modeled as distinct phenotypes. (B) A highly significant QTL, correlating with anophthalmia and microphthalmia, was detected in the middle of Chromosome 2, centered at 35 cM. (C) A suggestive QTL, correlating with coloboma of the fetal fissure, was detected on Chromosome 4. (D) A suggestive QTL, correlating with corneal lenticular adhesions, was detected on the proximal portion of Chromosome 2. (E) A suggestive QTL, correlating iridocorneal adhesions, was detected on Chromosome 12. (F) A suggestive QTL, correlating with PHPV, was detected on Chromosome 13.

Table 4
Agrn^{CFP} associated C57/BL/6J eye development QTLs

Phenotype	Chromosome	cM position	# Mice	LOD	% Dysgenic [a]
Anophthalmia/ microphthalmia	2	35 cM	20	3.40	100
Fetal fissure coloboma	4	65 cM	18	1.62	72
Lens cornea fusion	2	55 cM	23	1.95	95
Iris cornea fusion	12	5 cM	13	1.31	76
PHPV	13	0 cM	26	1.30	26

C57BL/6J loci segregating with specific types of ocular dysgenesis. Each type of dysgenesis is listed with its most significant QTL, the chromosome it was detected on, its centi-Morgan (cM) position and log of odds (LOD). The number of dysgenic mice with a given phenotype, and the percentage of these mice homozygous for C57BL/6J at the locus detected, are listed.

[a] The percentage of dysgenic mice carrying a locus was determined by dividing the number of mice that typed as homozygous C57BL/6J by the total number of mice with this phenotype at a given marker.

in our cross were categorized into one of six phenotypic categories: Group 1, anophthalmia and microphthalmia; Group 2, fetal fissure coloboma; Group 3, corneolenticular adhesions; Group 4, iridocorneal adhesions; Group 5, presence of PHPV; and Group 6, unaffected. Mice with multiple sub-phenotypes were included in multiple groups, for example if one eye was anophthalmic and the other eye had PHPV the mouse was included in both groups 1 and 5. Mice in groups 1–5 were analyzed compared to wild-type and dysgenic mice with different phenotypes (Figs. 7B–F). A highly significant association was found between mice in group 1 and a locus on Chromosome 2 (P value <0.001). N2 *Agrn*^{CFP2R9} mice homozygous for C57BL/6J alleles at this locus had a penetrance of anophthalmia or microphthalmia of 35%, close to the 40% of C57BL/6J *Agrn*^{CFP2R9} mice that have either of these phenotypes. Furthermore, all N2 anophthalmic or microphthalmic mice were homozygous C57BL/6J at this locus, while no mice heterozygous at this locus were anophthalmic or microphthalmic. The Chromosome 2 locus is in a 16 MB interval between the markers *rs3692748* and *rs3681694*. Suggestive associations were identified between phenotypic groups 2, 3, 4 and 5 and loci on Chromosomes 4, 2, 12 and 13, respectively (Table 4).

Discussion

This study demonstrates that the overexpression of agrin causes a spectrum of developmental eye defects. The defects are attributable to the agrin protein itself, as the penetrance is dose dependent and insensitive to the presence of the C-terminal CFP fusion or the integration site of the transgene. The optic stalk coloboma and subsequent misdifferentiation of the tissue as retina correlate with a paucity of SHH in the developing optic nerve. However, signaling systems beyond *Shh* are clearly affected, and not all mice show *Shh*-related defects.

Sensitivity of the C57BL/6J genetic background

Some of the phenotypic variability may be contributed by the C57BL/6J background, which is prone to spontaneous eye defects at a low frequency (Smith et al., 1994), and which provides a sensitized background for other factors that can affect the development of the eye, such as fetal alcohol exposure (Sulik et al., 1981). However, while the propensity for eye problems has been known for over 60 years (Chase, 1942), the low penetrance of these defects has made genetic mapping of the sensitizing loci impossible. Using, agrin overexpression as the developmental challenge, we have successfully mapped one strong sensitizing locus that predisposes C57BL/6J mice to anophthalmia. Interestingly, *Pax6* maps to this region, and *Pax6* mutations can cause microphthalmia and anophthalmia (Ashery-Padan and Gruss, 2001). Furthermore, expansion of PAX6 into the optic stalk occurred in *Agrn*^{CFP2R9} embryos that showed misdifferentiation of the optic nerve as retina, consistent with *Pax6* defects underlying both the *Agrn*-induced defects and the spontaneous defects in C57BL/6J. In preliminary tests of the possible involvement of *Pax6*, the *Agrn*^{CFP2R9} transgene was bred to a recessive *Pax6* allele, *JR4326*, (P.G.F. unpublished) in a C3H/HeBir genetic background. Eye defects were observed in all *Agrn*^{CFP2R9} F1 mice also heterozygous for the *Pax6* allele, while eyes were normal in all F1 mice carrying only the agrin transgene or only heterozygous for the *JR4326* locus (N25 mice examined). These results indicate that *Pax6* may sensitize the eye to defects induced by the agrin overexpression and are consistent with *Pax6* underlying the Chromosome 2 QTL.

Suggestive loci for other phenotypes may become significant with further study. Importantly, treating all defects as a single trait with varying severity did not reveal any significant linkage, while mapping modifier loci associated with distinct phenotypes (anophthalmia, PHPV, coloboma, etc.) gave significant results. This suggests that the sensitivity of C57BL/6J is polygenic. Multiple, distinct loci act to sensitize C57BL/6 to different, independent eye phenotypes. Of course, the modifiers identified are, by definition, those loci that sensitize C57BL/6J to agrin overexpression. However, the similarity of the eye defects in response to agrin overexpression and the spontaneous defects seen in C57BL/6J suggest that the same loci may be involved in the wild-type eye as well.

Agrin in the eye

Agrin is abundantly expressed in the wild-type eye and is a major heparan sulfate proteoglycan in the internal limiting membrane (Halfter, 1993; Halfter et al., 1997). This localization

to the ILM and other extracellular matrix structures, including blood vessels, is consistent with the observed localization of the transgenic agrin-CFP protein. In the chick eye, agrin is also reported to localize to glycinergic synapses in the retina (Mann and Kroger, 1996). Such a localization within the adult retina has not been observed in the transgenic mice. This may reflect species differences, antibody detection thresholds, or a dependence on the developmental stage examined.

The integrity of the ILM is essential for retinal–ganglion–cell axon-outgrowth and soma survival (Halfter et al., 2000, 2001, 2005). For instance, treatment with collagenase rapidly and irreversibly disrupts retinal morphology. The contribution of agrin to these functions of the ILM is unclear, but the lack of an eye phenotype at birth in the agrin loss-of-function mice suggests that any embryonic function must be redundant with other ILM components. Agrin does affect outgrowth of retinal axons (Halfter, 1996) and presynaptic differentiation (Campagna et al., 1995, 1997; Chang et al., 1997), and these effects depend in part on heparan sulfate (Baerwald-de la Torre et al., 2004).

HSPGs and developmental signaling in the eye

The variety of phenotypes caused by agrin overexpression is consistent with perturbations in the function of other HSPGs in eye development, which can have widely varying effects. The chemical modification of HS sulfonyl groups leads to defects in retinal axon targeting in *Xenopus* (Irie et al., 2002). The loss of HS-linked forms of perlecan results in postnatal lens degeneration in mice (Rossi et al., 2003). Mice lacking the heparan sulfate-2 sulfotransferase gene (*Hs2st1*) have an iris coloboma (Bullock et al., 1998), and mice lacking GlcNAc *N*-deacetylase/*N*-sulfotransferase 1 (*Ndst1*) have severe defects in eye development consistent with impaired SHH and FGF signaling.

Agrin directly interacts with FGF2, and this interaction affects neurite outgrowth (Cotman et al., 1999; Kim et al., 2003). HS also interacts directly with SHH, although this has not been demonstrated for agrin-associated HS chains (Rubin et al., 2002). Consistent with direct interaction, agrin overexpression decreases SHH in the developing optic nerve. The agrin-induced misdifferentiation of the optic nerve also resembles the phenotype of *Vax1*/*Vax2* mutant mice (Mui et al., 2005). The *Vax* genes control the PAX2/PAX6 boundary and are also downstream of *Shh*, further implicating *Shh* dysfunction in this aspect of the agrin overexpression phenotype. Furthermore, the *Vax* study showed that the differentiation of the optic stalk as the optic nerve requires the suppression of *Pax6* expression, which otherwise leads to retinal fate. This differentiation of the optic nerve as retina is therefore a default pathway and not dependent on signals from the surface ectoderm. Our results support this hypothesis, since the same phenotype occurs in the agrin transgenic mice by an independent manipulation.

It is noteworthy that agrin is localized to the structures in the eye that are adversely affected by overexpression, suggesting a direct role in the dysgenesis. However, it is also important to note that the phenotype is caused by overexpression, and eye defects are not observed in agrin knockout mice. Agrin overexpression may therefore be interfering with the interaction of other molecules to cause the phenotype. Such "non-specific" interactions are possible between HSPGs when the interactions are mediated by the HS groups and not by the core proteins. For example, loss of syndecan in *Drosophila* can be suppressed by overexpression of a glypican with a similar cellular localization (Johnson et al., 2004). Furthermore, agrin sometimes carries chondroitin sulfate modification in addition to heparan sulfate (Winzen et al., 2003), further increasing the number of molecular interactions that may be perturbed by agrin overexpression.

Therefore, we hypothesize that the defects we observed are, at least in part, caused by a perturbation in heparan sulfate function through agrin overexpression. The extent to which these effects depend on the agrin core protein for localization or the agrin gene for its expression pattern remain to be determined. However, it is an intriguing possibility that the overexpression of other HSPGs, particularly matrix bound proteins such as perlecan, may also cause defects in eye development.

Non-glycosaminoglycan interactions

The core protein of agrin also interacts with other extracellular molecules. Prominent among these interactions are α-dystroglycan, which interacts with the C-terminus of agrin (Campanelli et al., 1994; Gee et al., 1994; Gesemann et al., 1996; Hopf and Hoch, 1996), and the gamma1 chain of laminin trimers, which interacts with the N-terminus of agrin (Denzer et al., 1995; Kammerer et al., 1999). Disrupting the function of laminin or dystroglycan through the overexpression of agrin could also affect the development of the eye, as these proteins have recently been shown to be important, based upon loss-of-function studies (Lunardi et al., 2006; Zinkevich et al., 2006). Furthermore, mutations in glycosyltransferases that modify dystroglycan and eliminate its ability to interact with agrin also cause defects in the eye (Lee et al., 2005; Michele et al., 2002). Thus agrin's effects on eye development may extend beyond glycosaminoglycan interactions.

Agrin is a key signaling molecule for the formation of the neuromuscular junction. However, *in vivo* defects in neurodevelopment have been found only in the cholinergic synapses of the superior cervical ganglia in loss-of-function alleles of agrin (Gingras et al., 2002). The overexpression of agrin causes defects in eye development that resemble defects affecting HS synthesis or modification. The variability of the phenotype and the presence of multiple sensitizing loci in the C57BL/6J background suggest that multiple developmental events are affected by agrin overexpression. These effects could be through HS-overabundance, perturbed core–protein interactions, genetic predisposition, and even unknown environmental and epigenetic factors such as maternal or fetal stress. However, the high penetrance of defects in the sensitized C57BL/6J background and the well characterized biology of agrin make this system an excellent model for future studies on the molecular and genetic interactions that are needed for proper eye development.

Acknowledgments

We would like to thank Dr. J.H. Berden for his generous contribution of the GR14 anti-agrin antibody, Ellen Akeson and Dr. Lindsay Shopland for help in conducting FISH, Drs. Richard Smith and Patsy Nishina for a critical review of the manuscript, Weidong Zhang for assistance with QTL statistical analysis, and the Scientific Services of The Jackson Laboratory, particularly Histology and Imaging and Cell Biology and Microinjection. The monoclonal antibody ascites concentrates to NF and SHH developed by Dr. T.M. Jessell, and the monoclonal antibody to PAX6 developed by Dr. A. Kawakami were obtained from the Developmental Studies Hybridoma Bank developed under the auspices of the NICHD and maintained by The University of Iowa, Department of Biological Sciences, Iowa City, IA 52242. This research was funded by the National Eye Institute (EY-016031, RWB) and (EY-15966, PGF) and the Scientific Services of TJL are supported by CA34196 from the NCI.

Appendix A. Supplementary data

Supplementary data associated with this article can be found, in the online version, at doi:10.1016/j.ydbio.2006.11.033.

References

Ashery-Padan, R., Gruss, P., 2001. Pax6 lights-up the way for eye development. Curr. Opin. Cell Biol. 13, 706–714.

Baeg, G.H., Perrimon, N., 2000. Functional binding of secreted molecules to heparan sulfate proteoglycans in Drosophila. Curr. Opin. Cell Biol. 12, 575–580.

Baerwald-de la Torre, K., Winzen, U., Halfter, W., Bixby, J.L., 2004. Glycosaminoglycan-dependent and -independent inhibition of neurite outgrowth by agrin. J. Neurochem. 90, 50–61.

Bernfield, M., Gotte, M., Park, P.W., Reizes, O., Fitzgerald, M.L., Lincecum, J., Zako, M., 1999. Functions of cell surface heparan sulfate proteoglycans. Annu. Rev. Biochem. 68, 729–777.

Bullock, S.L., Fletcher, J.M., Beddington, R.S., Wilson, V.A., 1998. Renal agenesis in mice homozygous for a gene trap mutation in the gene encoding heparan sulfate 2-sulfotransferase. Genes Dev. 12, 1894–1906.

Bulow, H.E., Hobert, O., 2004. Differential sulfations and epimerization define heparan sulfate specificity in nervous system development. Neuron 41, 723–736.

Burgess, R.W., Skarnes, W.C., Sanes, J.R., 2000. Agrin isoforms with distinct amino termini: differential expression, localization, and function. J. Cell Biol. 151, 41–52.

Burgess, R.W., Dickman, D.K., Nunez, L., Glass, D.J., Sanes, J.R., 2002. Mapping sites responsible for interactions of agrin with neurons. J. Neurochem. 83, 271–284.

Campagna, J.A., Ruegg, M.A., Bixby, J.L., 1995. Agrin is a differentiation-inducing "stop signal" for motoneurons in vitro. Neuron 15, 1365–1374.

Campagna, J.A., Ruegg, M.A., Bixby, J.L., 1997. Evidence that agrin directly influences presynaptic differentiation at neuromuscular junctions in vitro. Eur. J. Neurosci. 9, 2269–2283.

Campanelli, J.T., Roberds, S.L., Campbell, K.P., Scheller, R.H., 1994. A role for dystrophin-associated glycoproteins and utrophin in agrin-induced AChR clustering. Cell 77, 663–674.

Chang, D., Woo, J.S., Campanelli, J., Scheller, R.H., Ignatius, M.J., 1997. Agrin inhibits neurite outgrowth but promotes attachment of embryonic motor and sensory neurons. Dev. Biol. 181, 21–35.

Chase, H.B., 1942. Studies on an anopthalmic strain of mice: III. Results of crosses with other strains. Genetics 27, 339–348.

Chow, R.L., Lang, R.A., 2001. Early eye development in vertebrates. Annu. Rev. Cell Dev. Biol. 17, 255–296.

Copeland, N.G., Jenkins, N.A., Court, D.L., 2001. Recombineering: a powerful new tool for mouse functional genomics. Nat. Rev., Genet. 2, 769–779.

Cotman, S.L., Halfter, W., Cole, G.J., 1999. Identification of extracellular matrix ligands for the heparan sulfate proteoglycan agrin. Exp. Cell Res. 249, 54–64.

Denzer, A.J., Gesemann, M., Schumacher, B., Ruegg, M.A., 1995. An amino-terminal extension is required for the secretion of chick agrin and its binding to extracellular matrix. J. Cell Biol. 131, 1547–1560.

Doerge, R.W., Churchill, G.A., 1996. Permutation tests for multiple loci affecting a quantitative character. Genetics 142, 285–294.

Fox, A.N., Zinn, K., 2005. The heparan sulfate proteoglycan syndecan is an in vivo ligand for the Drosophila LAR receptor tyrosine phosphatase. Curr. Biol. 15, 1701–1711.

Gee, S.H., Montanaro, F., Lindenbaum, M.H., Carbonetto, S., 1994. Dystroglycan-alpha, a dystrophin-associated glycoprotein, is a functional agrin receptor. Cell 77, 675–686.

Gesemann, M., Cavalli, V., Denzer, A.J., Brancaccio, A., Schumacher, B., Ruegg, M.A., 1996. Alternative splicing of agrin alters its binding to heparin, dystroglycan, and the putative agrin receptor. Neuron 16, 755–767.

Gingras, J., Rassadi, S., Cooper, E., Ferns, M., 2002. Agrin plays an organizing role in the formation of sympathetic synapses. J. Cell Biol. 158, 1109–1118.

Grobe, K., Inatani, M., Pallerla, S.R., Castagnola, J., Yamaguchi, Y., Esko, J.D., 2005. Cerebral hypoplasia and craniofacial defects in mice lacking heparan sulfate Ndst1 gene function. Development 132, 3777–3786.

Halfter, W., 1993. A heparan sulfate proteoglycan in developing avian axonal tracts. J. Neurosci. 13, 2863–2873.

Halfter, W., 1996. The behavior of optic axons on substrate gradients of retinal basal lamina proteins and merosin. J. Neurosci. 16, 4389–4401.

Halfter, W., Schurer, B., Yip, J., Yip, L., Tsen, G., Lee, J.A., Cole, G.J., 1997. Distribution and substrate properties of agrin, a heparan sulfate proteoglycan of developing axonal pathways. J. Comp. Neurol. 383, 1–17.

Halfter, W., Dong, S., Schurer, B., Osanger, A., Schneider, W., Ruegg, M., Cole, G.J., 2000. Composition, synthesis, and assembly of the embryonic chick retinal basal lamina. Dev. Biol. 220, 111–128.

Halfter, W., Dong, S., Balasubramani, M., Bier, M.E., 2001. Temporary disruption of the retinal basal lamina and its effect on retinal histogenesis. Dev. Biol. 238, 79–96.

Halfter, W., Willem, M., Mayer, U., 2005. Basement membrane-dependent survival of retinal ganglion cells. Invest. Ophthalmol. Visual Sci. 46, 1000–1009.

Holt, C.E., Dickson, B.J., 2005. Sugar codes for axons? Neuron 46, 169–172.

Hopf, C., Hoch, W., 1996. Agrin binding to alpha-dystroglycan. Domains of agrin necessary to induce acetylcholine receptor clustering are overlapping but not identical to the alpha-dystroglycan-binding region. J. Biol. Chem. 271, 5231–5236.

Inatani, M., Irie, F., Plump, A.S., Tessier-Lavigne, M., Yamaguchi, Y., 2003. Mammalian brain morphogenesis and midline axon guidance require heparan sulfate. Science 302, 1044–1046.

Irie, A., Yates, E.A., Turnbull, J.E., Holt, C.E., 2002. Specific heparan sulfate structures involved in retinal axon targeting. Development 129, 61–70.

Johnson, K.G., Ghose, A., Epstein, E., Lincecum, J., O'Connor, M.B., Van Vactor, D., 2004. Axonal heparan sulfate proteoglycans regulate the distribution and efficiency of the repellent slit during midline axon guidance. Curr. Biol. 14, 499–504.

Kammerer, R.A., Schulthess, T., Landwehr, R., Schumacher, B., Lustig, A., Yurchenco, P.D., Ruegg, M.A., Engel, J., Denzer, A.J., 1999. Interaction of agrin with laminin requires a coiled-coil conformation of the agrin-binding site within the laminin gamma1 chain. EMBO J. 18, 6762–6770.

Kantor, D.B., Chivatakarn, O., Peer, K.L., Oster, S.F., Inatani, M., Hansen, M.J., Flanagan, J.G., Yamaguchi, Y., Sretavan, D.W., Giger, R.J., Kolodkin, A.L., 2004. Semaphorin 5A is a bifunctional axon guidance cue regulated by heparan and chondroitin sulfate proteoglycans. Neuron 44, 961–975.

Kim, M.J., Cotman, S.L., Halfter, W., Cole, G.J., 2003. The heparan sulfate proteoglycan agrin modulates neurite outgrowth mediated by FGF-2. J. Neurobiol. 55, 261–277.

Lee, E.C., Yu, D., Martinez de Velasco, J., Tessarollo, L., Swing, D.A., Court, D.L., Jenkins, N.A., Copeland, N.G., 2001. A highly efficient Escherichia coli-based chromosome engineering system adapted for recombinogenic targeting and subcloning of BAC DNA. Genomics 73, 56–65.

Lee, J.S., von der Hardt, S., Rusch, M.A., Stringer, S.E., Stickney, H.L., Talbot, W.S., Geisler, R., Nusslein-Volhard, C., Selleck, S.B., Chien, C.B., Roehl, H., 2004. Axon sorting in the optic tract requires HSPG synthesis by ext2 (dackel) and extl3 (boxer). Neuron 44, 947–960.

Lee, Y., Kameya, S., Cox, G.A., Hsu, J., Hicks, W., Maddatu, T.P., Smith, R.S., Naggert, J.K., Peachey, N.S., Nishina, P.M., 2005. Ocular abnormalities in Large(myd) and Large(vls) mice, spontaneous models for muscle, eye, and brain diseases. Mol. Cell. Neurosci. 30, 160–172.

Lin, W., Burgess, R.W., Dominguez, B., Pfaff, S.L., Sanes, J.R., Lee, K.F., 2001. Distinct roles of nerve and muscle in postsynaptic differentiation of the neuromuscular synapse. Nature 410, 1057–1064.

Lunardi, A., Cremisi, F., Dente, L., 2006. Dystroglycan is required for proper retinal layering. Dev. Biol. 290, 411–420.

Mann, S., Kroger, S., 1996. Agrin is synthesized by retinal cells and colocalizes with gephyrin. Mol. Cell. Neurosci. 8, 1–13.

Michele, D.E., Barresi, R., Kanagawa, M., Saito, F., Cohn, R.D., Satz, J.S., Dollar, J., Nishino, I., Kelley, R.I., Somer, H., Straub, V., Mathews, K.D., Moore, S.A., Campbell, K.P., 2002. Post-translational disruption of dystroglycan–ligand interactions in congenital muscular dystrophies. Nature 418, 417–422.

Mui, S.H., Kim, J.W., Lemke, G., Bertuzzi, S., 2005. Vax genes ventralize the embryonic eye. Genes Dev. 19, 1249–1259.

Neumann, F.R., Bittcher, G., Annies, M., Schumacher, B., Kroger, S., Ruegg, M.A., 2001. An alternative amino-terminus expressed in the central nervous system converts agrin to a type II transmembrane protein. Mol. Cell. Neurosci. 17, 208–225.

Park, P.W., Reizes, O., Bernfield, M., 2000. Cell surface heparan sulfate proteoglycans: selective regulators of ligand–receptor encounters. J. Biol. Chem. 275, 29923–29926.

Perrimon, N., Bernfield, M., 2000. Specificities of heparan sulphate proteoglycans in developmental processes. Nature 404, 725–728.

Perrimon, N., Bernfield, M., 2001. Cellular functions of proteoglycans—an overview. Semin. Cell Dev. Biol. 12, 65–67.

Raats, C.J., Bakker, M.A., Hoch, W., Tamboer, W.P., Groffen, A.J., van den Heuvel, L.P., Berden, J.H., van den Born, J., 1998. Differential expression of agrin in renal basement membranes as revealed by domain-specific antibodies. J. Biol. Chem. 273, 17832–17838.

Rossi, M., Morita, H., Sormunen, R., Airenne, S., Kreivi, M., Wang, L., Fukai, N., Olsen, B.R., Tryggvason, K., Soininen, R., 2003. Heparan sulfate chains of perlecan are indispensable in the lens capsule but not in the kidney. EMBO J. 22, 236–245.

Rubin, J.B., Choi, Y., Segal, R.A., 2002. Cerebellar proteoglycans regulate sonic hedgehog responses during development. Development 129, 2223–2232.

Sanes, J.R., Lichtman, J.W., 1999. Development of the vertebrate neuromuscular junction. Annu. Rev. Neurosci. 22, 389–442.

Selleck, S.B., 2000. Proteoglycans and pattern formation: sugar biochemistry meets developmental genetics. Trends Genet. 16, 206–212.

Sen, S., Churchill, G.A., 2001. A statistical framework for quantitative trait mapping. Genetics 159, 371–387.

Shopland, L.S., Johnson, C.V., Byron, M., McNeil, J., Lawrence, J.B., 2003. Clustering of multiple specific genes and gene-rich R-bands around SC-35 domains: evidence for local euchromatic neighborhoods. J. Cell Biol. 162, 981–990.

Smith, R.S., Roderick, T.H., Sundberg, J.P., 1994. Microphthalmia and associated abnormalities in inbred black mice. Lab. Anim. Sci. 44, 551–560.

Stickens, D., Zak, B.M., Rougier, N., Esko, J.D., Werb, Z., 2005. Mice deficient in Ext2 lack heparan sulfate and develop exostoses. Development 132, 5055–5068.

Sulik, K.K., Johnston, M.C., Webb, M.A., 1981. Fetal alcohol syndrome: embryogenesis in a mouse model. Science 214, 936–938.

Take-uchi, M., Clarke, J.D., Wilson, S.W., 2003. Hedgehog signalling maintains the optic stalk–retinal interface through the regulation of Vax gene activity. Development 130, 955–968.

Turnbull, J., Powell, A., Guimond, S., 2001. Heparan sulfate: decoding a dynamic multifunctional cell regulator. Trends Cell Biol. 11, 75–82.

Winzen, U., Cole, G.J., Halfter, W., 2003. Agrin is a chimeric proteoglycan with the attachment sites for heparan sulfate/chondroitin sulfate located in two multiple serine–glycine clusters. J. Biol. Chem. 278, 30106–30114.

Zinkevich, N.S., Bosenko, D.V., Link, B.A., Semina, E.V., 2006. laminin alpha 1 gene is essential for normal lens development in zebrafish. BMC Dev. Biol. 6, 13.